Vulnerability Identification and Risk Tracing for Offshore Wind Power Integrated Power Systems

Yunhui Tan
College of Electrical Engineering, Shanghai University of Electric Power, Shanghai, China
2944792314@qq.com

Xiangjing Su
Offshore Wind Power Research Institute, Shanghai University of Electric Power, Shanghai, China
xiangjing_su@126.com

Shiqu Xiao
College of Electrical Engineering, Shanghai University of Electric Power, Shanghai, China
xiaoshiquovo@foxmail.com

Jiale Luo
College of Electrical Engineering, Shanghai University of Electric Power, Shanghai, China
770924331@qq.com

Shuai Yu
College of Electrical Engineering, Shanghai University of Electric Power, Shanghai, China
19186049960@163.com

Yang Fu
Offshore Wind Power Research Institute, Shanghai University of Electric Power, Shanghai, China
mfudong@126.com

***Abstract*—Modern power systems with large-scale offshore wind farms (OWFs) are frequently hit by typhoons, while the correlation between typhoon conditions and grid operational risks is unclear, making it difficult to conduct risk tracing analysis. This paper proposes a dynamic vulnerability identification model for power grids and constructs a Risk Propagation Graph (RPG). Firstly, dynamic centrality indices that couple topological structure with time-varying operational states are introduced to identify critical components. Then, Temporal Difference Index (TDI) and Cumulative Disturbance Index (CDI) are formulated to capture high-risk moments in typhoon periods. On this basis, the Power Transfer Distribution Factor (PTDF) is innovatively applied to the rapid analytical modeling of risk propagation in typhoon scenarios, achieving a path breakthrough from complex simulation to lightweight analysis. Finally, the effectiveness and superiority of the proposed model and method are analyzed and verified using a modified IEEE 30-bus system as an example.**

Keywords—Typhoon weather, Dynamic vulnerability identification, Risk propagation graph, Offshore wind power

I. Introduction

Large-scale offshore wind power integration is a key component in modern power systems, where the transmission channels are exposed to extreme marine weather such as typhoons, posing unprecedented challenges to grid security [1]. Typhoons can directly cause large-scale output reduction or even shutdown of wind turbines, seriously threatening the safe and stable operation of the power grid [2]. This poses a challenge for grid security analysis. Currently, the risk mechanisms between typhoon conditions and grid states are unclear, and the risk propagation process is difficult to characterize.

Regarding power grid risk assessment under extreme weather, scholars have conducted extensive research on vulnerability identification and risk propagation analysis. In terms of identifying system vulnerable components, traditional research employs static metrics based on complex network theory, among which betweenness centrality has been commonly applied due to its capability to measure the topological bridging role. Reference [3] developed a node importance assessment model based on complex network centrality theory to identify critical nodes in power grids. To make up for the deficiency of only considering the physical structure, Reference [4] proposed a flow betweenness metric, which incorporates line impedance into the complex network model, significantly improving the accuracy of critical node identification. Additionally, max-flow min-cut theory has been applied to identify static bottleneck sections that constrain the power transmission capability of systems [5]-[6]. Reference [5] employed a graph theory-based network flow algorithm for connectivity monitoring to identify critical transmission paths in power grids. Building on this, Reference [6] further introduced an improved maximum flow model for quantitatively assessing the structural vulnerability of power grids. However, these studies essentially belong to static analysis, In dynamic typhoon scenarios, the continuous power fluctuations of offshore wind farms cause the constant changes within grid states. This time-varying characteristics of the system make traditional static methods difficult to implement.

In terms of risk tracing analysis, existing researches focus on simulations of cascading failure models [7]-[9]. Reference [7] employed a spatiotemporal graph-based approach to analyze transmission line vulnerability in cascading failures. Reference [8] investigated line failure propagation characteristics under different attack scenarios using cascading failure network graphs. Meanwhile, Reference [9] proposed a pre-overload graph model capable of identifying risk correlations under load redistribution attacks. While such methods can reproduce the entire fault evolution process by simulating the continuous tripping of components, their computational burden is huge. Moreover, such "post-event" analysis is incapable for online diagnosis and monitoring. After identifying local vulnerabilities, a theoretical model should be established to quickly trace the paths and to depict an intuitive visual risk map for system operators.

In view of the shortcomings of current research, this paper proposes a set of analytical methods for identifying dynamic vulnerability and tracing risk propagation paths for large offshore wind integrated power systems under typhoon scenarios. Firstly, dynamic centrality indices that fuse real-time electrical states with temporal characteristics are introduced, enabling the precise localization of evolving risk origins. Then, innovatively, we circumvent computationally expensive cascading failure simulations by applying the Power Transfer Distribution Factor (PTDF) to construct a Risk Propagation Graph (RPG), achieving rapid, analytical visualization of risk diffusion paths. Finally, the effectiveness of the proposed method is verified through simulation analysis of a modified IEEE 30-bus example system.

II. Dynamic Identification of Power Grid Weak Points

A. Electrical Centrality Based Identification of Key Nodes

1) Electrical Betweenness Centrality

979-8-3315-8138-1

In power systems, power is not transmitted only along the shortest path. Therefore, using "betweenness" in graph theory to evaluate the importance of nodes and branches in the network is unreasonable. Electrical betweenness considers node capacity, transmission line impedance, and the weighted adjacency matrix, and can truly reflect the importance of nodes between generator and load node pairs.

The electrical betweenness of node *n* is defined as:

$$B_e^t(n) = \sum_{i\in G, j\in L} \sqrt{W_i^t W_j^t}\, B_{e,ij}^t(n) \tag{1}$$

where *G* is the set of generator nodes, *L* is the set of load nodes. (i, j) represents a generator-load node pair. W_i^t represents the weight of the generator node at time *t*, defined in this paper as the active output of generator *i* at time *t*, W_j^t is the load node weight, defined in this paper as the actual load of load *j* at time *t*. $B_{e,ij}^t(n)$ is the electrical betweenness contribution of node n for the generator-load node pair when a unit current is injected at time *t*. This electrical betweenness is normalized to obtain the following formula:

$$C_{be}^t(n) = \frac{B_e^t(n)}{\sum_{i\in G, j\in L} \sqrt{W_i^t W_j^t}} \tag{2}$$

2) Node Electrical Centrality

Eigenvector centrality is a topological graph metric used to quantify the centrality of nodes in a network. Its core idea can be summarized as: if a node is connected to other important nodes, then it is itself important. The eigenvector centrality of node *n* is defined as:

$$E_n^t = e_n^t = \frac{1}{\lambda}\sum_{j\in M(n)} e_j^t = \frac{1}{\lambda}\sum_{j=1}^{N} W_{nj}^t\, e_j^t \tag{3}$$

where *M*(n) is the set of nodes directly connected to node n, *N* is the total number of nodes in the entire network.

The obtained electrical betweenness centrality and eigenvector centrality are fused to obtain the Node Electrical Centrality (NEC) that can reflect the node's electrical characteristics and topological importance. The NEC of node *i* is defined as:

$$NEC^t(i) = \mu C_{be}^t(i) + (1-\mu)E_i^t \tag{4}$$

B. Max-Flow Theory Based Identification of Key Lines

1) Transmission Bottlenecks Based on Max-Flow

At any time *t*, we abstract the power grid as a large complex network composed of nodes and edges. Buses with generators and loads can be regarded as nodes in the network, and transmission lines can be regarded as edges, represented by graph $G = (V, E)$, where the set *V* contains *n* nodes, and the set *E* contains *k* edges. The adjacency matrix *A* is used to define the connectivity of the graph, and the element a_{ij} represents the weight of the edge connecting node *i* and node *j*. This paper selects the transmission line capacity as the edge weight.

The essence of the max-flow problem is to find the maximum transmission flow from source node *s* to sink node *t*. The Edmonds-Karp algorithm is used to solve the max-flow in graph *G*. This algorithm uses Breadth-First Search (BFS) to find augmenting paths, stop extending when the contribution of the newly added branch to the system max-flow is less than 1% of the current max-flow, with a time complexity of $O(VE^2)$, making it suitable for dynamic analysis of power grids.

Through this algorithm, the corresponding to time *t* minimum cut set $C_{\min}(t)$ and the flow of the lines $f_k(t)$ can be obtained. The lines in the minimum cut set are defined as the key transmission bottleneck lines of the onshore grid at time *t*, denoted as $L_c(t) = \{k \mid k \in C_{\min}(t)$. Because it does not take into account Kirchhoff's laws and line impedance, it is not applicable to scenarios that require precise analysis of power flow direction, voltage stability, or complex circulation. In cases where the transmission capacity risk is dominant due to a typhoon, this model can serve as an effective preliminary analysis tool, and its results should be combined with electrical indicators based on power flow.

2) Maximum Flow Centrality Considering Source-Load

To comprehensively evaluate the bottleneck role of a single line in the entire network, it is necessary to accumulate its contribution in the propagation paths of all source-sink pairs. For this purpose, a maximum flow centrality index considering source-load weights is proposed, defined as follows:

$$C_k^t = \sum_{u\in G, v\in L} \sqrt{W_u^t W_v^t} \cdot \delta_k(t) \cdot f_k^{uv}(t) \tag{5}$$

$\delta_k(t)$ takes the value 1 when line *k* belongs to the minimum cut set, otherwise it is 0. Use the maximum flow $f_{\max}^t$ at time *t* to normalize C_k^t:

$$\overset{*}{C_k^t} = \frac{C_k^t}{\sum_{u\in G, v\in L} \sqrt{W_u^t W_v^t}\, f_{max}^t} \tag{6}$$

C. Temporal Characteristics Based Identification of High-Risk Moments

This paper constructs two core temporal characteristic indicators: Temporal Difference Index (TDI) and Cumulative Disturbance Index (CDI), to identify high-risk moments.

TDI is used to measure the abrupt change degree of grid vulnerability between adjacent moments, calculating the TDI values for all key nodes and key lines in the entire network respectively. Taking lines as an example, their Temporal Difference Index at time *t* is defined as follows:

$$I_{TDI}^t = \sum_{k=1}^{N_L} \mid C_k^t - C_k^{t-1} \mid \tag{7}$$

where N_L is the total number of lines in the system, C_k^t represents the centrality index at time *t*.

At time *t*, the system's Cumulative Disturbance Index is defined as:

$$I_{CDI}^t = \sum_{\tau=t_0}^{t} \left(\frac{1}{N_L}\sum_{k=1}^{N_L} C_k^{\tau}\right) \tag{8}$$

III. Construction of Power Grid Risk Propagation Graph Based on Power Transfer Distribution Factor

A. Basic Principle of Power Transfer Distribution Factor

In power systems, power injection changes at any node will affect the power flow of lines in the system. The Power Transfer Distribution Factor (PTDF) is a linearized indicator that describes the degree of impact of node power disturbances on the power flow of lines across the network. Its core advantage is that it is calculated directly based on the grid topology and parameters, without the need for iterative simulation, adapting to the needs of online rapid analysis under typhoon scenarios. The linear relationship between active power flow and node power injection can be expressed :

$$P_{\text{flow}} = M^{\text{non-ref}}[PBP_{22}]^{-1}P_{\text{inj}}^{\text{non-ref}}$$
$$= H'P_{\text{inj}}^{\text{non-ref}} = (0 \quad H')\begin{pmatrix} P_{\text{inj}}^{\text{ref}} \\ P_{\text{inj}}^{\text{non-ref}} \end{pmatrix} = HP_{\text{inj}} \qquad (9)$$

where P_{flow} represents the change in branch active power flow when node power injection changes, P_{inj} represents the bus active power injection, H represents the PTDF matrix considering the reference bus.

Select the high-risk moment t identified in Chapter II, starting from the key lines and key nodes, by applying disturbances to the node injection power, and using the PTDF matrix, the line power flow changes can be quickly obtained, yielding the next risk line. If multiple risk lines appear, the line with the highest risk degree is selected as the next risk line. This paper uses the load loss rate η=30% is adopted as the stop criterion for risk chain tracing. This threshold is set based on engineering practices related to the *N-1* and *N-k* security criteria for power system operation and analysis of historical incidents where systems approached the critical point of uncontrollable load shedding. The formation algorithm of the risk chain is shown in Fig. 1.

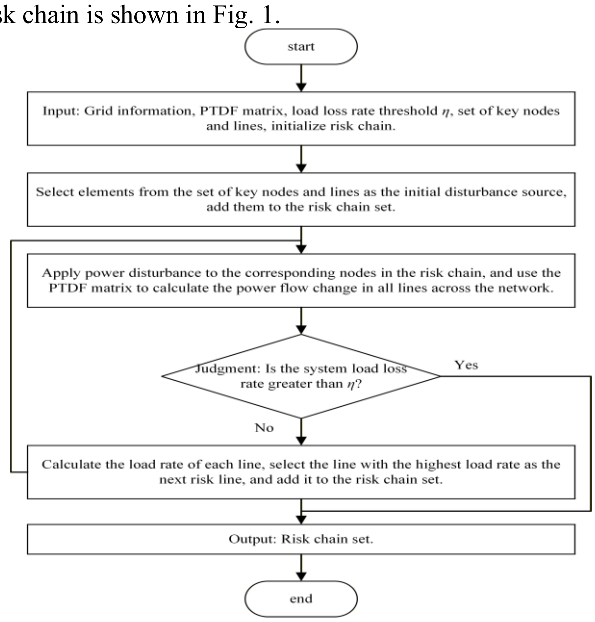

Fig. 1 Risk chain formation algorithm

B. *Construction Method of Risk Propagation Graph*

For a risk chain $R = \{L_1, L_2, \cdots, L_n\}$, take L_1 as the nodes in the topological graph, i.e., $V = \{L_i | i = 1,2,\cdots,n\}$, take the sequential order of risk development between lines as the edges of the topological graph, i.e., $E = \{e_j | e_j = L_j L_{j+1}, j = 1,2,\cdots,n-1\}$, take the centrality index of the end node L_{j+1} connected to edge e_j as the weight of that edge, then the risk chain can be represented by a directed weighted graph $R = \{V, E\}$.

Suppose there are m risk chains, $R_j = \{V^j, E^j\}(j = 1,2,\cdots,m)$, then the RPG can be represented as:

$$R_N = \{(V,E) \mid V = V^1 \cup V^2 \cup \cdots \cup V^m,$$
$$E = E^1 \cup E^2 \cup \cdots \cup E^m\} \qquad (10)$$

When synthesizing multiple risk chains into an RPG, line overlaps may occur. In this case, the weight of edge e_j is defined as follows:

$$W = \sum_{j=1}^{h} \frac{1}{n^j} w^j \qquad (11)$$

where h represents the number of overlapping lines in each risk chain, n^j represents the number of line elements in the j risk chain, w^j represents the weight of edge e_j in the corresponding risk chain.

IV. Case Studies

A. *Case System and Related Parameter Description*

To verify the effectiveness of the proposed method for identifying dynamic vulnerability and tracing risk propagation paths of the power grid under typhoon scenarios, a modified IEEE 30-bus system is selected as the basic topology structure for the case study. The specific system wiring diagram is shown in Fig. 2. Node 1 is the onshore AC grid slack bus, node 31 is connected to a wind farm with a rated capacity of 1100MW, and is integrated into the AC grid at node 5 via the flexible DC grid-connected system. Buses 8 and 13 are connected to an onshore wind farm and a PV power plant, respectively, raising the share of renewable energy integration in the system to 45%. This paper uses the landing simulation of Typhoon "Bebinca" as the typhoon scenario. The typhoon's continuous impact time is 3 days.

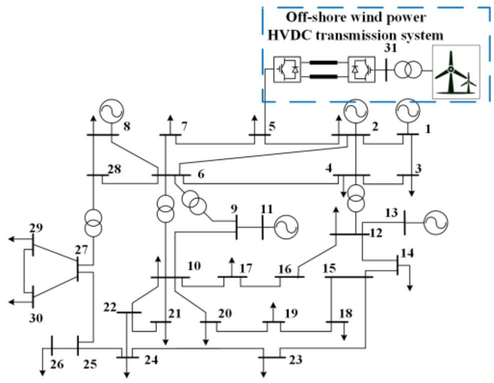

Fig. 2 Diagram of modified IEEE 30 bus test system

B. *Analysis of Dynamic Weak Point Identification Results in the Power Grid*

The time-series power injection from the offshore wind farm can yield time-series power flow results. Using the power flow algorithm as in [10], the time-series values of the state variables of the onshore grid at a 15-minute time scale are obtained as input for subsequent analysis.

1) *Analysis of Dynamic Key Node Identification Results*

At a certain point, the ranking of the electrical centers is shown in Fig 3. It can be seen that the electrical centrality of each node varies greatly. This indicates that different nodes have different significance in the power transmission of the grid. The differences in node electrical centrality are the result of the interaction between the node's position in the network topology and its transmission capacity. The maximum node electrical centrality is for node 6 (0.984), and the minimum is for node 26 (0.036). This is because node 6 is not only located at the connection point of two transformers but also connected to two generator nodes, occupying an important position in the overall topology. In contrast, node 11 is only connected to one generator and one load, making it relatively isolated in the entire AC grid, resulting in a lower comprehensive electrical centrality.

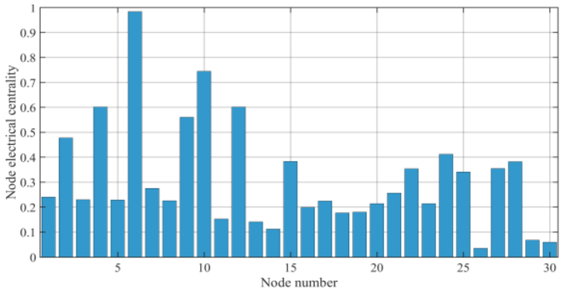

Fig. 3 Node Electrical Centrality

In the time-series scenario, sources and loads will continue to change due to the typhoon's impact, so the weight of each node will be affected and change. The importance of nodes may change at different times. Table I shows the top 5 nodes in terms of electrical centrality and their centrality values at different times t, as well as the results from another static identification model in the literature.

TABLE I
RANKING OF CENTRALITY AT DIFFERENT TIME POINTS

t=285		t=286		t=287		Other model	
Node	NEC	Node	NEC	Node	NEC	Node	NEC
6	0.982	6	0.955	6	0.955	6	0.397
10	0.734	10	0.761	10	0.760	10	0.360
4	0.592	12	0.631	12	0.631	22	0.313
12	0.574	9	0.597	4	0.597	12	0.298
9	0.537	4	0.596	9	0.596	4	0.289

Compared with the static model, the dynamic identification results in Table 3 highlight the importance of introducing source-load characteristics for accurately identifying key nodes. In the model of this paper, the rankings of nodes 4, 9, and 12 alternate at different times. This fluctuation directly reflects the drastic changes in wind farm injection power and the real-time adjustment of onshore loads during the typhoon process, which alter the power distribution and key propagation paths across the network. In contrast, the static model has a fixed ranking, and node 22 ranks high due to its pure topological importance. The dynamic model can capture this operating state-dependent vulnerability, thus more realistically reflecting the time-varying origin of power grid risks during the typhoon process.

2) Analysis of Dynamic Key Line Identification Results

Fig. 4 shows the identification results of key lines in the power grid at the peak moment of typhoon landfall.

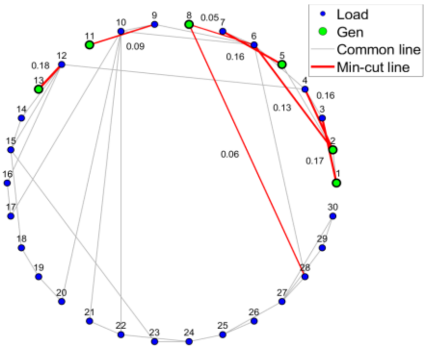

Fig. 4 Key line distribution

In Fig. 4, green represents generator nodes, and blue represents load nodes. To completely disconnect the generator and load nodes, the minimum cut set composed of red lines is obtained. This represents the transmission capacity bottleneck of the power grid. The weight of a line in the minimum cut set represents the proportion of that edge's flow in the maximum flow. The larger the weight, the greater the impact of disconnecting this line on the power grid, so it is used as the basis for judging the importance of the line. Table II presents a comparison between the critical lines identified by this method and the line loading rates calculated based on [10]. It can be observed that the critical lines identified by the max-flow min-cut approach largely align with the high-load lines in the power-flow results. Although line 2-5 exhibits a relatively high loading rate, it is not a critical transmission path between sources and loads, and therefore is not classified as a critical line in this work.

TABLE II
COMPARISON OF CRITICAL LINE IDENTIFICATION RESULTS AND LINE LOADING RATES

Max-Flow Min-Cut Identification Results	Line Weight	Criticality Ranking from Power Flow Calculation	Line Loading Rate
12-13	0.186	12-13	0.881
5-7	0.163	5-7	0.863
2-4	0.145	2-5	0.849
1-3	0.139	2-4	0.846
6-8	0.136	1-3	0.841
2-6	0.098	6-8	0.838

3) Analysis of High-Risk Moment Identification Results

Based on the Temporal Difference Index and Cumulative Disturbance Index, the high-risk moments during the 3-day typhoon impact are calculated, and the results are shown in Fig. 5.

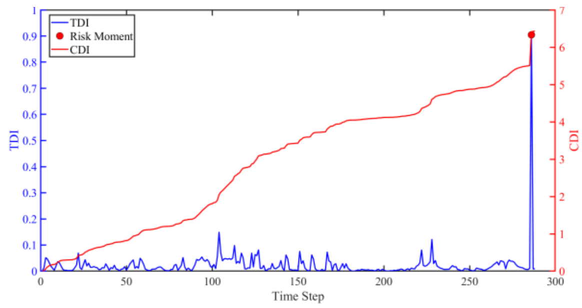

Fig. 5 Time-series curves of grid TDI and CDI and high-risk moments

The abrupt changes in the TDI and CDI indices in Fig. 5 accurately capture the risk accumulation process of the power grid. Before t=285, the CDI rises gently, indicating that the grid vulnerability is accumulating slowly. At t=285 to 286, the TDI shows a sharp peak, and simultaneously, the slope of the CDI curve increases sharply, which is a clear signal of a high-risk moment. This coincides perfectly in time with the actual grid-connected capacity, indicating that this identification method can effectively respond to major disturbance events occurring within the system. To quantify the detection performance of TDI and CDI, a high-risk moment is defined as when the instantaneous fluctuation rate of offshore wind power output, $V_{Pw} = |P(t) - P(t-1)|/P\_rated$, reaches 15%. A threshold γ is set, and a moment is considered high-risk when TDI(t) > γ. A sensitivity analysis on γ is conducted to quantify the performance in terms of missed detection rate and false alarm rate, as detailed in Figure 6.

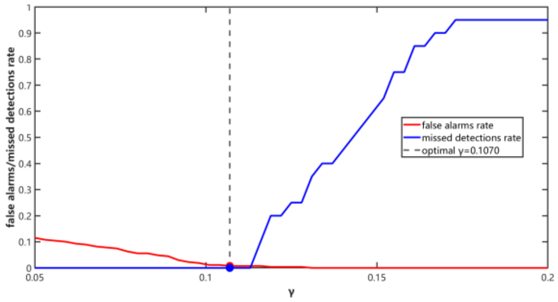

Fig. 6 Threshold γ sensitivity analysis

As shown in Figure 6, when the threshold $\gamma < 0.1$, the false alarm rate is relatively high while the missed detection rate is 0. When $\gamma > 0.12$, the false alarm rate is low but the missed detection rate gradually increases. When the threshold γ equals 0.107, the false alarm rate is 0.74% and the missed detection rate is 0, which is the optimal value.

C. *Risk Propagation Graph Construction Results*

Using the high-risk moments and key weak points of the power grid identified in section *B* as the starting points of power grid risk, and selecting a load loss rate threshold η=30%, the constructed RPG is shown in Fig. 7. In the subsequent analysis, nodes refer to risk lines. Unless otherwise specified, risk lines are referred to as nodes when discussing the RPG.

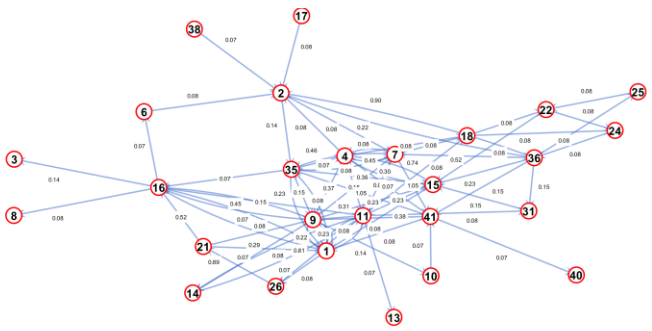

Fig. 7 Risk Propagation Graph of key weak points

From Fig. 7, it can be seen that the RPG can reflect the direction and mechanism of risk propagation in the power grid. The distribution of node out-degree and in-degree in the figure reveals two different risk roles: high out-degree nodes are risk amplifiers or propagation sources. Once they fail, they widely spread disturbances to other parts of the system, while high in-degree nodes are risk convergence points or victims, easily implicated by faults in other lines in the system. In terms of defense strategies, strengthening real-time monitoring and protection of high out-degree nodes can more effectively prevent the initial spread of risk while taking preventive control measures for high in-degree nodes can improve the anti-impact capability of that area.

To verify the validity of the risk propagation model based on PTDF, this study compared the risk propagation chain derived from the PTDF analysis method with the simulation results of the power flow and cascading failures based on detailed time-domain simulation. Five high-risk moments during the typhoon period were selected, and multiple key weak points were chosen as the starting points to form risk propagation chains as test cases. The results showed that in over 90% of the cases, the first three core risk lines identified by the two methods and their propagation sequence were highly consistent. The method in this paper only took 1.21 seconds, while the cascading failure simulation required 12.76 seconds.

V. Conclusion

This paper proposes a dynamic vulnerability identification model and a risk propagation tracing method for large offshore wind integrated power systems under typhoon disasters. A dynamic electrical centrality index incorporating time-varying operational states is constructed, enabling more accurate identification of time-sensitive weak spots in the power grid. This method achieves a superior success rate of 99.26% in identifying high-risk moments. Furthermore, by leveraging the PTDF to deduce risk chains and construct a RPG, the model enables rapid simulation of spatiotemporal risk propagation, benefiting from its linearized computational advantage. This approach supports online analysis and early warning, effectively overcoming the limitations of traditional cascading failure simulations.

Acknowledgment

This work is supported by National Key R&D Program of China “Remote monitoring and fault diagnosis technology for offshore wind power grid connected systems (2023YFB2406900)”.

References

[1] J. He, Z. Hu, Y. Liu, Z. Bao and Y. Zhu, "Dispatch Strategy for the Power System With Large Offshore Wind Power Integration Under a Typhoon: A Two-Stage Sample Robust Optimization Approach," IEEE Transactions on Industry Applications, vol. 61, no. 3, pp. 4636-4648, May-June 2025.

[2] Y. Liu, S. Li, P. W. Chan and D. Chen, "On the Failure Probability of Offshore Wind Turbines in the China Coastal Waters Due to Typhoons: A Case Study Using the OC4-DeepCwind Semisubmersible," IEEE Transactions on Sustainable Energy, vol. 10, no. 2, pp. 522-532, April 2019.

[3] Xu Lin,Wang Xiu-li,Wang Xi-fan. Electric Betweenness and Its Application in Vulnerable Line Identification in Power System. Proceedings of the CSEE,2010,Vol.30(1): 33-39.

[4] B. Liu, Z. Li, X. Chen, Y. Huang and X. Liu, "Recognition and Vulnerability Analysis of Key Nodes in Power Grid Based on Complex Network Centrality," IEEE Transactions on Circuits and Systems II: Express Briefs, vol. 65, no. 3, pp. 346-350, March 2018.

[5] T. Werho, V. Vittal, S. Kolluri and S. M. Wong, "Power System Connectivity Monitoring Using a Graph Theory Network Flow Algorithm," IEEE Transactions on Power Systems, vol. 31, no. 6, pp. 4945-4952, Nov. 2016.

[6] J. Fang, C. Su, Z. Chen, H. Sun and P. Lund, "Power System Structural Vulnerability Assessment Based on an Improved Maximum Flow Approach," IEEE Transactions on Smart Grid, vol. 9, no. 2, pp. 777-785, March 2018.

[7] Y. Liu, S. Gao, J. Shi, X. Wei and Z. Han, "Sequential-Mining-Based Vulnerable Branches Identification for the Transmission Network Under Continuous Load Redistribution Attacks," IEEE Transactions on Smart Grid, vol. 11, no. 6, pp. 5151-5160, Nov. 2020.

[8] X. Wei, J. Zhao, T. Huang and E. Bompard, "A Novel Cascading Faults Graph Based Transmission Network Vulnerability Assessment Method," IEEE Transactions on Power Systems, vol. 33, no. 3, pp. 2995-3000, May 2018.

[9] Y. Liu, S. Gao, J. Shi, X. Wei, Z. Han and T. Huang, "Pre-Overload-Graph-Based Vulnerable Correlation Identification Under Load Redistribution Attacks," in IEEE Transactions on Smart Grid, vol. 11, no. 6, pp. 5216-5226, Nov. 2020.

[10] ZHOU Tao，CHEN Zhong，DAI Zhongjian，et al. Power flow algorithm for AC/DC system with VSC-MTDC. Proceedings of the CSEE，2019，39（11）：3140-3148.